ELSEVIER

Journal of Nuclear Materials 290–293 (2001) 715–719

journal of nuclear materials

www.elsevier.nl/locate/jnucmat

Consistency check of Z_{eff} measurements in ergodic divertor plasmas on Tore Supra

B. Schunke *, C. DeMichelis, R. Guirlet, P. Monier-Garbet, M. Mattioli, E. Chareyre, O. Meyer

Association Euratom-CEA sur la Fusion Controlée, CEA Cadarache, DRFC-SIPP, Batiment 507, 13108 St.-Paul-Lez-Durance, France

Abstract

On Tore Supra, the mean effective charge Z_{eff} of the plasma is deduced routinely from line integrated measurements of visible Bremsstrahlung. In order to get a deeper understanding of this measurement, and to obtain high confidence in the data, we have compared the visible Bremsstrahlung data to line radiation of impurities present in the plasma, removing any error from the processing technique. The paper presents a systematic study of the correlation between the Z_{eff} derived from the two methods, and the dependence on plasma parameters and geometrical factors. A good correlation is found, independent of the position of the outboard pump limiter (OPL). However, the fitting parameter of the empirical method is different for different plasma currents, due to the variation of the emission profiles. The agreement between the two methods is good, confirming the role of carbon and oxygen as the main impurities in the Tore Supra tokamak.

Keywords: Experimental techniques; Plasma properties; Impurity; Carbon

1. Introduction

Reliable determination of the mean effective charge (Z_{eff}) of the plasma is of the highest importance for impurity control in fusion devices. On Tore Supra, reliable Z_{eff} measurements allow to assess the performance of the ergodic divertor (ED) in terms of impurity screening capability, particularly during injection of impurities such as neon, argon and nitrogen. The plasma Z_{eff} is routinely deduced from line integrated measurements of visible Bremsstrahlung. This standard method is generally reliable, but it has been suspected that certain discharge scenarios lead to systematic errors in the measurement, and therefore to over- or under-estimation of the actual value of Z_{eff}. For example, systematically lower Z_{eff} values were found in discharges with advanced outboard pump limiter (OPL). Common error sources of the Bremsstrahlung method include errors in the input data (electron density n_e, electron temperature T_e, magnetic flux surfaces), error in the Gaunt factor, calibration errors, unidentified line radiation and blackbody radiation. An alternative approach is to deduce Z_{eff} from spectroscopic observations of impurity radiation present in the plasma. Analysis of the coherence of the data bases and the consistency of the data, particularly taking into account the Bremsstrahlung measurements from all available sight lines, allows to gauge systematic errors of both methods and also yields information about the chemical composition of the plasma.

2. Experimental set-up

On Tore Supra, visible Bremsstrahlung is observed with eight poloidal viewing lines (Fig. 1) and one tangential viewing line (not shown) in a narrow wavelength interval, observing a well-defined, restricted plasma volume [1]. The detection system consists of a telescope, which focuses the incoming light onto eight optical fibres mounted in a single array, an optical interference filter and a registration system consisting of photomultipliers

* Corresponding author. Tel.: +33-4 42 25 62 02, fax: +33-4 42 25 49 90.

E-mail address: schunke@drfc.cad.cea.fr (B. Schunke).

0022-3115/01/$ - see front matter
PII: S0022-3115(00)00450-5

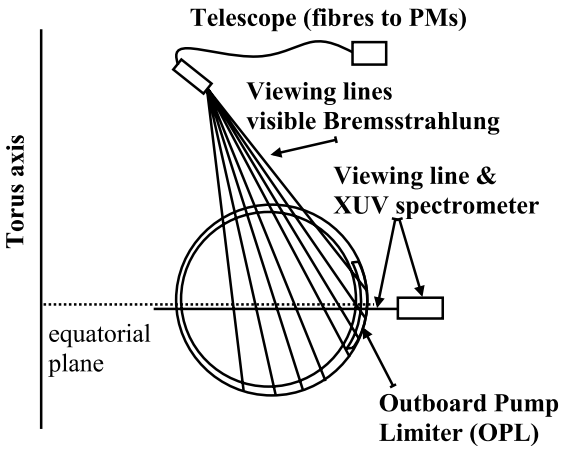

Fig. 1. Viewing lines of Z_{eff} and XUV diagnostics on Tore Supra.

operated in counting mode, an ICM100 card, and the central TS data storage system. The central wavelength of the interference filter is 523.8 nm with a spectral bandwidth of 1 nm, which corresponds to the impurity-line free region in Tore Supra. The diagnostic is located in the proximity of the Thomson scattering diagnostic, which measures the n_e and T_e profiles necessary to derive the Z_{eff}. All fibres end in individual PMs and acquisition channels, allowing for redundant measurements. The toroidal viewing line uses an in situ fibre and can be prone to reduced transmission due to a coating being deposited on the entrance lens. It was therefore excluded from this analysis. The code which provides the Z_{eff} for the database uses the density profiles measured by the Interferometer and the Thomson scattering and the temperature profiles provided by Thomson scattering and heterodyne radiometry. Fig. 1 also shows the sightline of the absolutely calibrated XUV spectrometer SIR [2], which traverses the major radius of the plasma just below the mid-plane. The spectrometer consists of a converted Schwob–Fraenkel spectrograph of 2 m-grating radius operated at extreme grazing incidence (1.5°) angle. It is equipped with a holographic grating of 600 grooves/mm. Two microchannel plate detectors are movable along the Rowland circle, and cover 4 nm each between 1 and 33 nm. Observed spectral lines in the XUV include Lyman alpha ($L\alpha$) of carbon and oxygen, CuXIX, FeXV, NiXVIII, ArXVI and NeX. For other elements, a VUV spectrometer can be used to complement the data.

3. Description of the analysis approach

The Z_{eff} value is derived from the line integrated measurement of the observed Bremsstrahlung in the usual way [3]:

$$Z_{\text{eff}} = \frac{\lambda}{0.95 \times 10^{-13}} \times \int \frac{B_{\text{brems}}}{G_{\text{ff}}(T_e, Z_{\text{eff}}) \cdot n_e^2(r) T_e^{-1/2}(r)}\, dr \quad (1)$$

with B_{brems} measured Bremsstrahlung signal, g_{ff} Gaunt factor, n_e electron density, and T_e electron temperature taken preferentially from the Thomson scattering diagnostic. Alternatively, the Zeff value can be derived from the density of the impurities present in the plasma via their line radiation:

$$Z_{\text{eff}} = \sum_i \frac{n_i Z_i (Z_i - 1)}{n_e} + 1, \quad (2)$$

where Z_i is the atomic number and n_i is the impurity density. The impurity densities can be written as expressions of the measured intensities with $I = (1/4\pi) P_{\text{EC}} n_e n_z L$ (P_{EC} is the photo emission coefficient of the considered transition of the emitting ion species z, n_z the density of the observed ionisation state, L the integration length over the radiating region). An exact treatment requires the observation of all impurity species and the inclusion of all line contributions in Eq. (2). In a first step, we concentrated on the contributions of the weighted sum of the observed OVIII and CVI intensities. These ionisation stages are found inside the confined plasma and are therefore representative of the central impurity densities of these species. The P_{EC}s were taken from the database ADAS [4]. For the range of electron temperatures and densities of Tore Supra plasmas, this reduces (2) to:

$$Z_{\text{eff}} = 1 + f \cdot \lfloor I_{CVI}/n_e^2 + I_{OVIII}/n_e^2 \rfloor, \quad (3)$$

where the factor f in front of the brackets is to be determined by linear regression analysis. Note that the factor f accounts for the numerical coefficients for the two terms in the parenthesis and also for the variation in P_{EC}s and the calibration of the spectrometer.

4. Measurements

The fitting parameter f from the simple expression (3) was computed for a large database of deuterium ergodic divertor discharges of the experimental campaign 1999, sorted into data-sets with equal plasma and divertor currents and OPL position, etc. The analysis concentrated on the flat top current phase, selecting all discharges for which a full set of diagnostic data was available (Z_{eff}, T_e, n_e, impurity data). The discharges analysed ranged from 2 to 5×10^{19} m^{-3} central n_e and 1–2.5 keV central T_e, and from 1 to 3×10^{18} m^{-3} n_e and 10–90 eV T_e in the divertor as measured by a Langmuir probe, which is located in the equatorial plane of the vacuum vessel (Fig. 1). Linear regression analysis results

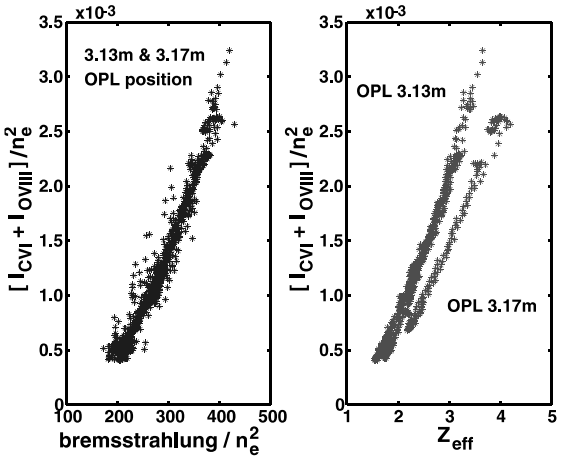

Fig. 2. Correlation between: (a) spectroscopic and Bremsstrahlung measurement, and (b) spectroscopic measurement and Z_{eff} for different OPL positions.

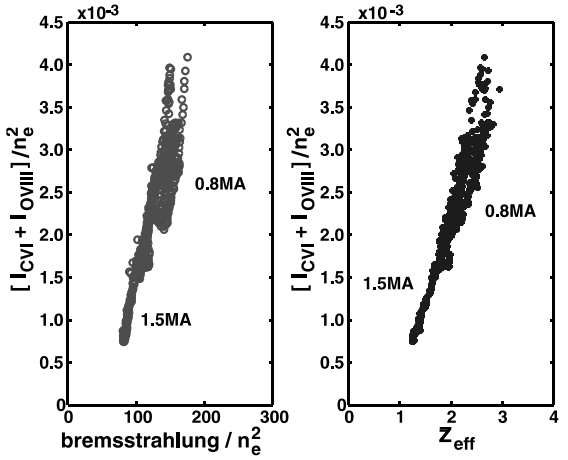

Fig. 3. Correlation between: (a) spectroscopic and Bremsstrahlung measurement, and (b) spectroscopic measurement and Z_{eff} for varying I_{p}.

in surprisingly small residues, and therefore errors, for the analysed data-sets, showing that the simple analysis approach chosen is valid for a large number of discharges. Different viewing lines of the Bremsstrahlung diagnostic required different fitting factors, but generally the central viewing lines of the poloidal system are in good agreement, while the outer ones may detect stray light for some scenarios.

Fig. 2 shows the correlation between the weighted sum of the carbon and oxygen signals and the measured Bremsstrahlung signal normalised to the square of the linear density (a) and the derived Z_{eff} (b), for a series of ergodic divertor shots with a plasma current of 1.5 MA, a divertor current of 45 kA, but two positions of the outboard pump limiter at 3.13 and 3.17 m. A good correlation for the Bremsstrahlung signal is found, while for Z_{eff} the data fall on two distinctive curves; for each OPL position a different fitting factor is required to describe the correlation. This hints at an underlying problem with the plasma geometry when the OPL is used, which enters the Z_{eff} in the calculation: if the density and temperature profiles are not very well defined due to errors in the magnetic flux geometry, errors are transmitted to the calculated Z_{eff}. For data-sets with different plasma currents (Fig. 3), different fitting factors are found for the Bremsstrahlung as well as the Z_{eff} correlation. This effect is real and not an artefact of the data processing. To exclude possible systematic errors in the Z_{eff} database affecting the analysis, the spectroscopic data were directly correlated to the Bremsstrahlung normalised by the square of the density, ignoring the weak T_{e} dependence.

Fig. 4(a) shows the fitting factor f as a function of plasma current at constant divertor current, and (b) as a function of auxiliary heating (ICRH power). The fitting

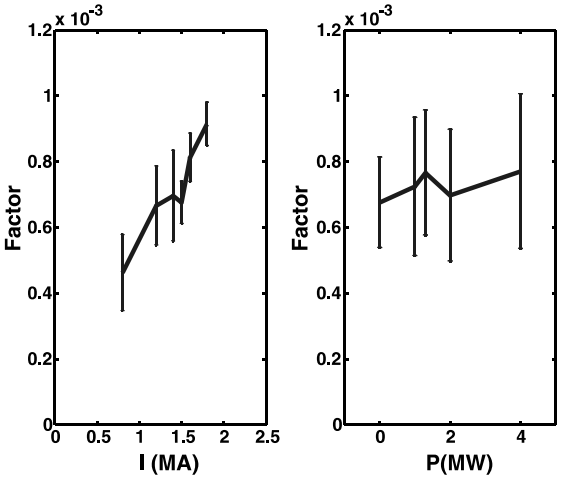

Fig. 4. Dependence of fitting parameter f on plasma current and auxiliary heating.

factor rises with plasma current, but stays constant if auxiliary heating is applied. The dependence on the plasma current can be due to a variation of the emission profiles due to varying T_{e} profiles, and therefore an effect of the divertor, or due to varying n_{e} profiles and an effect of transport. Better understanding of the empirical method, and an investigation of the effects of the density profiles and transport, requires the utilisation of an impurity transport code.

5. Transport analysis

To understand the dependence of the fitting parameter f on the plasma current, two discharges with 1.6

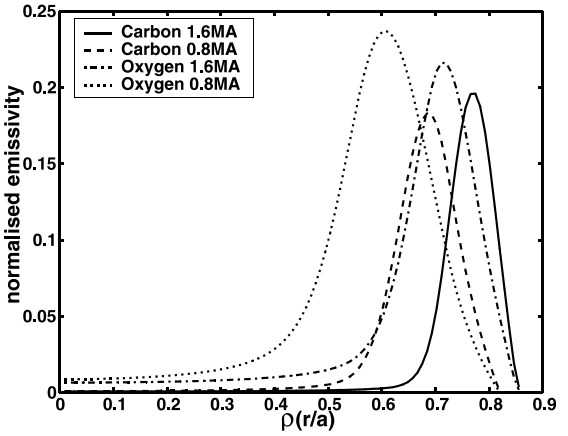

Fig. 5. Carbon and oxygen emission profiles for discharges at 0.8 and 1.6 MA.

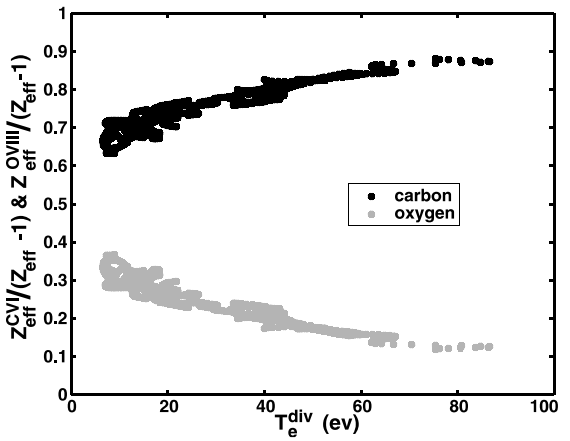

Fig. 6. Relative contribution of carbon and oxygen from the $L\alpha$ emission to the total Z_{eff}.

and 0.8 MA plasma current, but the same OPL position, same minor radius, same toroidal field, have been analysed using the Tore Supra 1-D impurity transport code [5]. The impurity code describes ionisation, recombination and radial transport of the ions of a given impurity species in cylindrical geometry. Both time-dependent as well as stationary versions of the code are available. Input parameters into the code are the electron temperature and density profiles, $T_e(r)$ and $n_e(r)$, and the thermal neutral deuterium profile, $n_D(r)$. Both diffusive and convective terms are included in the impurity flux. Running the transport code iteratively allowed to obtain the concentrations of C and O impurities by adjusting the central impurity densities to be consistent with the Z_{eff} and the radiated power. It was found that the emission profiles of the $L\alpha$ lines of carbon and oxygen were different for different plasma currents. Fig. 5 shows the distribution of the $L\alpha$ emission of carbon and oxygen for the two discharges at 0.8 and 1.6 MA. Note that the normalised emissivities shown are normalised to the maximum emissivity of each impurity species. The absolute concentrations were found to be 2.11% C and 0.53% O for the 1.6 M discharge, and slightly larger, 2.43% C and 0.61% O for the 0.8 MA discharge, which can be explained by the lower electron density in the discharge with the lower current.

6. Further results

The analysis was extended to include further terms in the sum of impurities (Cu, Fe, Ni, Cl) in (2). It was found, however, that their contributions were small, and that the fit did not improve significantly. Therefore, they were consequently disregarded in the analysis. The only discharges benefiting from an additional term in the sum were discharges with extrinsic impurity injection, such as neon or argon. In these discharges the measured NeX or Ar XVI intensities were comparable to those of the carbon and oxygen signals, and taking into account their contributions by including a third term reduced the residuals in the regression.

The ratio of the observed carbon to oxygen intensities in the Tore Supra ergodic divertor discharges analysed varied from 2.5 to 12, depending on conditioning history and additional heating. Nevertheless, the simple approach above holds for a large database of ED discharges independent of the ratio of carbon and oxygen. Using the fitting parameter obtained from the regression analysis, the contribution of carbon and oxygen to the total Z_{eff} can be established. Fig. 6 shows the fractions of the spectroscopic Z_{eff}s for carbon and oxygen over the Z_{eff} from the Bremsstrahlung measurement as a function

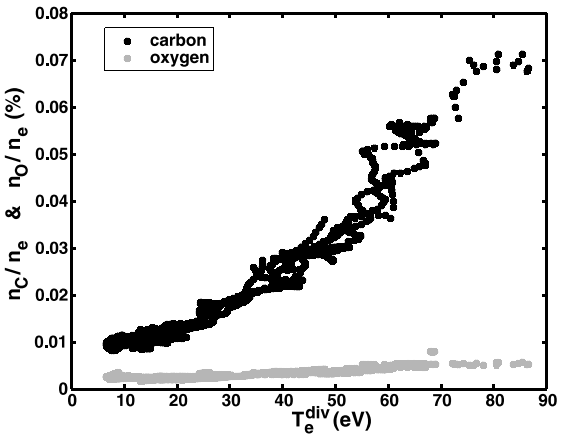

Fig. 7. Carbon and oxygen density normalised to the electron density.

of the divertor temperature. Carbon provides the dominant contribution to the spectroscopic Z_{eff} for all divertor temperatures, the contribution of oxygen reduces with increasing divertor temperature. Carbon remains the dominant impurity in Tore Supra, and the absolute density increases with increasing divertor temperature (Fig. 7). This is in agreement with expectation as physical sputtering is the main carbon production mechanism contributing to the plasma pollution [6]. Both radiation enhanced sublimation and chemical sputtering can produce localised carbon concentrations, but, due to their low penetration efficiency, do not contribute to the core carbon content.

7. Conclusions

The Z_{eff} measured by Bremsstrahlung was compared to a Z_{eff} derived from the weighted sum of $L\alpha$ emission of the dominant intrinsic impurities. This simple empirical approach works well for a large database of ergodic divertor discharges. In the experimental 1999 campaign, the main contributors to the Z_{eff} in Tore Supra ergodic divertor plasmas were the light impurities carbon and oxygen, with the ratio of C and O depending on the actual vessel and discharge conditions, but carbon being the dominant contribution for all discharges. Other impurities, such as metals, contribute only a small fraction to the total Z_{eff} and can therefore be neglected.

References

[1] S. Boeddeker, Private communication (Z_{eff} in Tore Supra, Association EURATOM-CEA Report NT Φ 129, 1998).
[2] C. Breton et al., Mater. Sci. Technol. 1 (1990) 50.
[3] K. Kadota et al., Nucl. Fus. 20 (1980) 209.
[4] H.P. Summers, Atomic Data and Analysis Structure User Manual, JET Report IR(94) 06, JET Joint Undertaking, Abingdon, 1994.
[5] M. Mattioli et al., Nucl. Fus. 38 (1998) 1629.
[6] S.J. Tobin et al., Plasma Phys. Control Fus. 40 (1998) 1335.